Diverging Thermal Expansion of the Spin-Ladder System $(C_5H_{12}N)_2CuBr_4$

T. Lorenz,[1,][*] O. Heyer,[1] M. Garst,[2] F. Anfuso,[2] A. Rosch,[2] Ch. Rüegg,[3] and K. Krämer[4]

[1]*II. Physikalisches Institut, Universität zu Köln, Zülpicher Straße 77, 50937 Köln, Germany*

[2]*Institut für Theoretische Physik, Universität zu Köln, Zülpicher Straße 77, 50937 Köln, Germany*

[3]*London Centre for Nanotechnology and Department of Physics and Astronomy, University College London,
London WC1E 6BT, United Kingdom*

[4]*Department of Chemistry and Biochemistry, University of Bern, Freiestrasse, CH−3000 Bern 9, Switzerland*

(Received 9 November 2007; published 15 February 2008; publisher error corrected 19 February 2008)

We present high-resolution measurements of the $c^\star$-axis thermal expansion and magnetostriction of piperidinium copper bromide $(C_5H_{12}N)_2CuBr_4$. The experimental data at low temperatures are well accounted for by a two-leg spin-ladder Hamiltonian. The thermal expansion shows a complex behavior with various sign changes and approaches a $1/\sqrt{T}$ divergence at the critical fields. All low-temperature features are semiquantitatively explained within a free-fermion model; full quantitative agreement is obtained with quantum Monte Carlo simulations.

In recent years there has been an increasing interest in spin compounds exhibiting magnetic field-induced quantum phase transitions. Examples are a Bose-Einstein condensation of magnons [1,2] studied in three-dimensional (3D) systems like coupled spin dimers [3–5] or arrays of coupled spin-1 chains [6,7] or spin-ladders [8,9]. These systems share a zero-field ground state with a spin gap. In a magnetic field two quantum phase transitions are present; at H_{c1} the gap closes and at H_{c2} the fully field-polarized state is reached. An interesting scenario arises in the limit of very weakly coupled ladders or chains where an extended temperature regime controlled by 1D physics is expected. The low-dimensionality makes the investigation of quantum critical properties particularly exciting, and the thermal expansion α is especially suited for this purpose. In fact, it has been shown that the Grüneisen parameter $\Gamma = \alpha/C$, where C is the specific heat, necessarily diverges at a quantum phase transition [10]. In addition, α shows a sign change whose location in the phase diagram indicates accumulation of entropy [11]. For $D < 1/\nu$, where ν is the correlation length exponent, even α will diverge at criticality. For a spin-ladder, $\nu = 1/2$, the thermal expansion at the critical fields is expected to behave as $\alpha \sim 1/\sqrt{T}$ [10]. Experimentally, this is largely unexplored due to the lack of suitable model materials.

In this letter we present a study of the thermal expansion and the magnetostriction of single crystalline piperidinium copper bromide $(C_5H_{12}N)_2CuBr_4$ whose magnetic subsystem is a very good realization of a two-leg spin ladder [8] with Hamiltonian

$$\mathcal{H} = \sum_{i=1}^{N}[J_\perp \mathbf{S}_{i,1}\mathbf{S}_{i,2} + J_\parallel(\mathbf{S}_{i,1}\mathbf{S}_{i+1,1} + \mathbf{S}_{i,2}\mathbf{S}_{i+1,2}) - g\mu_B H(S_{i,1}^z + S_{i,2}^z)]. \tag{1}$$

The critical fields $H_{c1} = 6.8$ T and $H_{c2} = 13.9$ T imply $J_\perp/k_B = 12.9$ K and $J_\parallel/k_B = 3.6$ K for the rung and leg

couplings, respectively [12]. The interladder couplings are very weak since no indications of three-dimensional magnetic ordering are present down to $T \simeq 100$ mK [15]. On approaching each of the critical fields, we find highly anomalous temperature dependencies of α. For $0.3\text{K} \lesssim T \lesssim 2$ K, $\alpha(T)$ approaches $1/\sqrt{T}$ divergences with opposite signs for H_{c1} and H_{c2} in agreement with the expected quantum critical behavior. Away from the critical fields, α shows a complex structure with various sign changes, essentially antisymmetric with respect to $(H_{c1} + H_{c2})/2$. All these low-temperature features are reproduced semiquantitatively within a model of free fermions, although the latter is valid only close to $H_{c1/c2}$.

$(C_5H_{12}N)_2CuBr_4$ crystallizes in a monoclinic structure [14]. The legs of the spin ladders are oriented along the a axis and the rungs roughly ($\approx 20°$) along $c^\star$. The single crystals used in this study have been grown from solution [15]. We present high-resolution measurements of the thermal expansion $\alpha(T) = 1/L_0\partial\Delta L(T)/\partial T$, magnetostriction $\varepsilon(H) = \Delta L(H)/L_0$ and its field derivative $\lambda = \partial\varepsilon(H)/\partial H$. Here, L_0 is the sample length along $c^\star$; $\Delta L(T)$ and $\Delta L(H)$ denote the temperature- and field-induced change at constant H and T, respectively. The measurements have been performed on a home-built capacitance dilatometer in magnetic fields $H \parallel c^\star$ up to 17 T for $0.3\text{K} \lesssim T \lesssim 10$ K.

Figure 1 displays $\varepsilon(H)$ measured at various constant temperatures. At $T = 335$ mK, $\varepsilon(H)$ is field independent up to about 6 T; then it continuously increases until it saturates for $H \gtrsim 15$ T. This behavior strongly resembles that of the low-temperature magnetization [8]. The inset of Fig. 1 shows the magnetostriction coefficient $\lambda(H)$ with two pronounced peaks at 335 mK, whose magnitude shrink with increasing temperature until around 2 K both peaks merge into one broad plateau which further broadens towards higher T. In order to identify the critical fields specified above we used linear interpolations of the peak positions of $\lambda(H)$ towards $T = 0$ K.
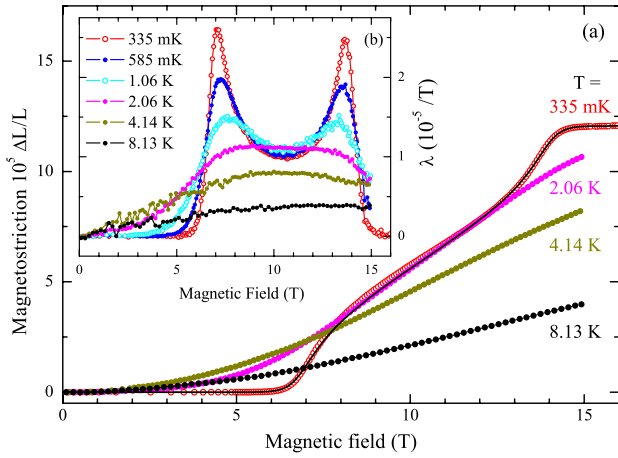
FIG. 1 (color online).   (a) Magnetostriction $\varepsilon = \Delta L(H)/L$ and (b) $\lambda = \partial \varepsilon / \partial H$ measured along $c^\star$. The solid line in (a) is a fit of ε at 335 mK within a free-fermion model.

FIG. 2 (color online).   Thermal expansion $\alpha = 1/L \partial L/\partial T$ measured along the $c^\star$ direction in various magnetic fields (a) below H_{c1}, (b),(c) between H_{c1} and H_{c2}, and (d) above H_{c2}. Note the logarithmic temperature scale. The dashed line in (a) is a fit with the Schottky formula Eq. (2). The arrows signal the order of the $\alpha(T)$ curves with increasing field.

In Fig. 2(a) we summarize the thermal expansion data for $H \lesssim H_{c1}$. In zero field, $\alpha(T)$ has a pronounced peak around 5 K followed by a strong increase above about 15 K. The latter is due to the usual thermal expansion of phononic origin, while the 5 K peak is well described by a Schottky formula indicating the thermal occupation of triplet excitations, see discussion below. These degenerate triplets are split upon increasing magnetic field which is reflected in a broadening and slight shift of the Schottky peak towards lower T. For $H \gtrsim 5.5$ T, the magnitude of the peak starts to grow until around H_{c1} a continuous increase of $\alpha(T)$ down to our lowest $T \simeq 0.3$ K is observed. For $H > H_{c1}$, this low-T increase rapidly weakens and α becomes even negative for $H = 7.2$ T; see Fig. 2(b). With further increasing field this sign change shifts towards higher T and a clear minimum-maximum structure of $\alpha(T)$ becomes visible, whose amplitude continuously decreases until a comparatively featureless $\alpha(T)$ curve is reached at the aforementioned symmetry field $(H_{c1} + H_{c2})/2 = 10.4$ T. On approaching H_{c2} we observe the same systematics of $\alpha(T)$ but with inverted signs, Fig. 2(c); in particular, a negative Schottky peak develops above H_{c2}; see Fig. 2(d).

We now turn to the theoretical discussion of the magnetic contributions to the thermal expansion and magnetostriction arising from the Hamiltonian (1). As $J_\parallel/J_\perp \approx 1/4$ for $(C_5H_{12}N)_2CuBr_4$ we can resort to the strong coupling limit $J_\parallel \ll J_\perp$ where the physics emerges in a transparent way. In this limit, the Hamiltonian (1) represents a sum of weakly interacting dimers in one dimension. For $k_B T \gg J_\parallel$, the magnetic contribution to α is then attributed to the thermal occupation of single-dimer states described by the Schottky formula

$$\alpha_{Sch} = \frac{\gamma e^{\beta(h+J_\perp)}[h(1 - e^{2\beta h}) + J_\perp(1 + e^{\beta h} + e^{2\beta h})]}{k_B T^2 (1 + e^{\beta h} + e^{2\beta h} + e^{\beta(h+J_\perp)})^2}, \quad (2)$$

where $1/\beta = k_B T$ and $\gamma = \frac{1}{V_D} \frac{\partial J_\perp}{\partial p}$ with the volume per

dimer $V_D \simeq 859$ Å^3 [15]. A fit for $H = 0$ [dashed line in Fig. 2(a)] yields $\gamma \simeq 11.7 \times 10^{-5}$ [16] implying a uniaxial pressure, $p_{c^\star} \parallel c^\star$, dependence $\partial \ln J_\perp / \partial p_{c^\star} \simeq 55\%/GPa$. In lowest order, the leg coupling leads to a mean-field shift of the effective magnetic field, $h = g \mu_B H - J_\parallel M/(g \mu_B)$, where M is the magnetization of a single dimer. The Schottky formula (2) accounts well for the field dependence of the 5 K peak (not shown). In particular, it identifies for any given temperature a unique magnetic field where the thermal expansion vanishes and changes sign, see Fig. 3. Upon decreasing temperature, the positions of vanishing α in the (H, T) phase diagram shift to lower fields towards the location of the singlet-triplet transition, $h \simeq J_\perp$.

However, when temperature is of order $k_B T \simeq J_\parallel$ the behavior changes qualitatively and the Schottky formula ceases to be valid. In contrast to a simple singlet-triplet level crossing of isolated dimers, the kinetic energy of the triplet excitations gives rise to an extended gapless phase at zero temperature terminated by two quantum critical points at $H_{c1/c2}$. In the low-T limit $k_B T \ll J_\perp$, the Hamiltonian (1) can be mapped onto an effective XXZ spin-1/2 chain [17–19] that is described by interacting tight-binding Jordan-Wigner fermions with bandwidth $J_\parallel$ and chemical potential tuned by magnetic field, $\mu = g \mu_B H - J_\perp + \mathcal{O}(J_\parallel)$. Here, the magnetic field and the pressure-dependent $J_\perp(p)$ only enter via the chemical potential μ which implies essentially the same behavior
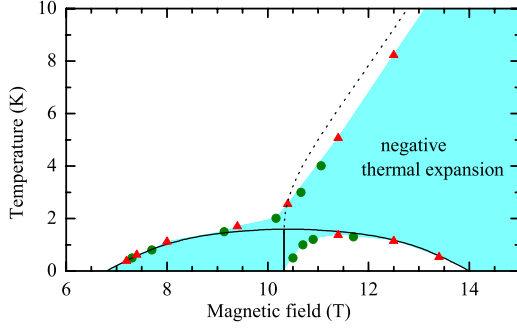
FIG. 3 (color online).   Regions of positive and negative thermal expansion α along the $c^\star$ axis of $(C_5H_{12}N)_2CuBr_4$. The triangles and circles denote the positions of vanishing α determined from an interpolation along the T and H axis, respectively. In the shaded area α is negative. The dashed line indicates the zeros of α as predicted by the Schottky formula (2). The solid lines show zeros of α derived from the free-fermion fitting formula (4), which for $T = 0$ start at the two quantum critical points located at $H_{c1} = 6.8$ T and $H_{c2} = 13.9$ T and at $(H_{c1} + H_{c2})/2$. Note that a crossing point of lines of zeros as suggested by Eq. (4) is not realized as the regions of negative α are connected.

for the derivatives of the free energy with respect to H and p. This not only explains the close correspondence between magnetization [8] and $\varepsilon(H)$ of Fig. 1 in the low-T limit but it also provides an intuitive interpretation of the various sign changes of the thermal expansion α.

The sign change of thermal expansion, $\alpha \propto \partial S/\partial p$, reveals the locations of extrema of entropy, S, in the phase diagram that originate from the proliferation of low-energy fluctuations close to a quantum critical point [11]. In the present context, the close vicinity of two quantum critical points $H_{c1/c2}$ gives rise to a rich structure in α, see Fig. 2, whose sign changes we summarized in Fig. 3. At elevated temperatures, thermodynamics is not able to resolve the distance between the critical points, viz., the bandwidth $J_\parallel$ of triplet excitations. For temperatures $J_\parallel < k_B T \ll J_\perp$, this is reflected in a broad single peak in the entropy as a function of magnetic field $S(H)$, or, equivalently, as a function of the chemical potential μ, indicating the singlet-triplet level crossing. This peak implies a single sign change of $\alpha \propto \partial S/\partial J_\perp \propto \partial S/\partial \mu$ in agreement with the prediction of the Schottky formula (2). At $k_B T \simeq J_\parallel$, however, thermodynamics starts to resolve the triplet bandwidth which is reflected in a splitting of the entropy peak into two separate maxima whose positions approach the critical points $H_{c1/c2}$ for $T \to 0$ K. The bifurcation of the entropy peak is the origin of the rich structure of α. The two maxima and the enclosed minimum of $S(H)$ result in three consecutive sign changes of $\alpha(H)$ for $k_B T \lesssim J_\parallel$ as shown in Fig. 3.

Close to criticality, $H \approx H_{c1/c2}$ and $k_B T \ll J_\parallel$, the interactions among Jordan-Wigner fermions can be neglected and the critical model reduces to free non-relativistic fermions. The resulting singular part of the free energy has the scaling form
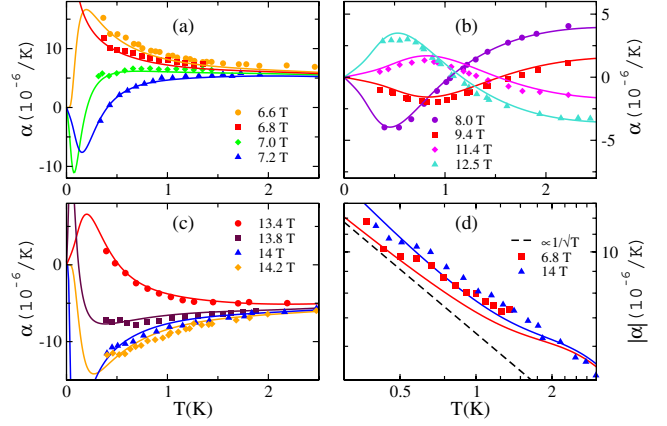
FIG. 4 (color online).   Panels (a)–(c) compare representative experimental data (symbols) of $\alpha(T)$ to theoretical curves (lines) obtained within the free-fermion model (4). All these curves are fully determined by $H_{c1/c2}$ and a factor γ obtained from a fit to $\varepsilon(H)$ data at $T = 335$ mK (see Fig. 1). Panel (d) shows the thermal expansion near $H_{c1/c2}$ on a double-logarithmic scale together with the limiting $1/\sqrt{T}$ behavior (dashed line).

$$F_{\mathrm{cr},n} = |g\mu_B(H - H_{cn})|^{3/2}\phi_n\left(\frac{k_B T}{g\mu_B(H - H_{cn})}\right), \quad (3)$$

where $n = 1, 2$ label the two distinct critical points and the scaling function ϕ was specified in [20]. Assuming that the critical fields $H_{c1/c2}$ are smooth functions of pressure, it follows from (3) that $\varepsilon(H) \propto \partial F_{\mathrm{cr},n}/\partial p \propto \partial F_{\mathrm{cr},n}/\partial H_{cn}$ approaches the same characteristic square root behavior as the magnetization in the zero temperature limit, $\varepsilon(H) \sim \sqrt{|H - H_{cn}|}$; this is already apparent in the low-T data in Fig. 1. For the critical thermal expansion the previously announced divergence $\alpha \sim 1/\sqrt{T}$ is found for $|H - H_{cn}| \ll T$. Note that a divergent thermal expansion at a quantum critical point is not prohibited by any fundamental principle. However, (3) also predicts a divergent critical contribution to the compressibility that might result in a preemptive first-order transition of the elastic system [21].

In order to capture the complex behavior of $\alpha(T, H)$ for $k_B T < J_\parallel$ we employ a simple fitting formula

$$\alpha_{\mathrm{FF}} = -\gamma \int_{-\pi}^{\pi} \frac{dk}{2\pi} \frac{(\mu - \epsilon_k)}{4k_B T^2 \cosh^2((\mu - \epsilon_k)/(2k_B T))}, \quad (4)$$

where $\mu = g\mu_B(2H - H_{c1} - H_{c2})/2$, the dispersion $\epsilon_k = \frac{1}{2}g\mu_B(H_{c2} - H_{c1})\cos(k)$, and γ measures the pressure dependence of the singlet-triplet crossing field, $\gamma = g\mu_B(\partial(H_{c1} + H_{c2})/\partial p)/(2V_D)$. Formula (4) follows from a free-fermion model with a pressure dependent chemical potential μ and dispersion ϵ_k; note that it reproduces the qualitatively correct $1/\sqrt{T}$ behavior close to the critical fields. The fit of $\varepsilon(H)$ at 335 mK, see Fig. 1, identifies $\gamma \simeq 12 \times 10^{-5}$ with the saturation value of $\varepsilon(H)$ at large fields, in good agreement with the value obtained from the Schottky fit of $\alpha(T)$. Having γ fixed, Eq. (4) strikingly reproduces the complex behavior of $\alpha(T)$
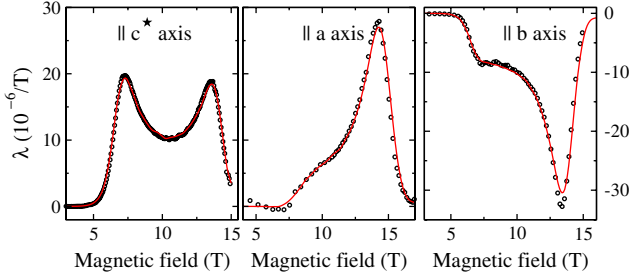
FIG. 5 (color online). Anisotropic magnetostriction coefficients λ (symbols) measured along $c^\star$, a, and b. The lines are quantum Monte Carlo fits using the experimental values of $J_\perp$ and $J_\parallel$ and two additional parameters for each direction, which measure the uniaxial pressure dependencies of $J_\perp$ and $J_\parallel$ [22].

in the low-T limit for all magnetic fields without further adjustment of any parameter, see Fig. 4. In particular, Eq. (4) confirms the three consecutive sign changes of α at lowest T as discussed above. The fit also demonstrates in Fig. 4(a) that in the measured temperature range the off-critical curve at $H = 6.6$ T is even larger than the critical one at $H_{c1} = 6.8$ T, but is expected to cross the latter at lower T. In Fig. 4(d) we show the $\alpha(T)$ curves that are closest to the two critical fields on a double-logarithmic scale. Whereas α at $H = 6.8$ T is critical, the one at $H = 14$ T is slightly off critical. The dashed line indicates the limiting $1/\sqrt{T}$ behavior. The deviation of the latter from the critical $H = 6.8$ T fitting curve (solid line) is attributed to certain corrections to scaling that are still sizeable in the considered temperature range; note, however, that the simplistic formula (4) does not correctly capture these corrections. The small offset between the experimental data and the fit in Fig. 4(d) amounts to a systematic error in the effective prefactor γ at criticality of $\simeq 10\%$ [22].

Figure 5 compares the uniaxial magnetostriction coefficient λ along the $c^\star$ axis with the ones along the orthogonal a and b directions. While the former is nearly symmetric with respect to $(H_{c1} + H_{c2})/2$ this symmetry is missing in the other two directions. This difference is due to the additional contribution arising from the pressure dependence of the leg coupling $J_\parallel$. It turns out that the dependence of $J_\parallel$ on uniaxial pressure $p_{c^\star} \parallel c^\star$ is very weak, $|\partial J_\parallel / \partial p_{c^\star}| \ll |\partial J_\perp / \partial p_{c^\star}|$, such that its influence can be neglected. The single dominant $p_{c^\star}$-dependent energy scale $J_\perp$ causes peaks in λ at $H_{c1/c2}$ that are of comparable sizes as $\partial H_{c1}/\partial p_{c^\star} \approx \partial H_{c2}/\partial p_{c^\star} \propto \partial J_\perp/\partial p_{c^\star}$ [12]. This is not the case for the orthogonal directions where the respective uniaxial pressure dependencies of $J_\perp$ and $J_\parallel$ are of similar magnitudes. In particular, the small relative size of the peaks at $H_{c1} \approx (J_\perp - J_\parallel)/g\mu_B$ can be understood as a partial cancellation of the two pressure dependencies $\partial J_\parallel/\partial p_n \sim \partial J_\perp/\partial p_n$ yielding a small $\partial H_{c1}/\partial p_n$, with $n = a$, b. Taking the pressure dependencies of both, $J_\perp$ and $J_\parallel$, into account, we find excellent quantitative

agreement with quantum Monte Carlo simulations of the Hamiltonian (1), solid lines in Fig. 5 [22].

In summary, we measured the magnetostriction and thermal expansion of $(C_5H_{12}N)_2CuBr_4$. For both physical quantities we find excellent agreement with calculations based on a two-leg spin-ladder Hamiltonian (1). The thermal expansion α is critically enhanced as $1/\sqrt{T}$ close to the two quantum critical points at $H_{c1/c2}$ and shows various sign changes as a function of H and T signaling entropy extrema in the phase diagram. This complex behavior of α is semiquantitatively explained within a model of free fermions, and we find quantitative agreement with quantum Monte Carlo calculations.

*lorenz@ph2.uni-koeln.de
 [1] I. Affleck, Phys. Rev. B **41**, 6697 (1990).
 [2] T. Giamarchi and A. M. Tsvelik, Phys. Rev. B **59**, 11 398 (1999).
 [3] Ch. Rüegg *et al.*, Nature (London) **423**, 62 (2003).
 [4] N. Johannsen *et al.*, Phys. Rev. Lett. **95**, 017205 (2005).
 [5] T. Lorenz *et al.*, J. Magn. Magn. Mater. **316**, 291 (2007).
 [6] V. S. Zapf *et al.*, Phys. Rev. Lett. **96**, 077204 (2006).
 [7] S. A. Zvyagin *et al.*, Phys. Rev. Lett. **98**, 047205 (2007).
 [8] B. C. Watson *et al.* Phys. Rev. Lett. **86**, 5168 (2001).
 [9] V. O. Garlea *et al.*, Phys. Rev. Lett. **98**, 167202 (2007).
[10] L. Zhu *et al.*, Phys. Rev. Lett. **91**, 066404 (2003).
[11] M. Garst and A. Rosch, Phys. Rev. B **72**, 205129 (2005).
[12] The coupling constants can be determined perturbatively from the critical fields. Up to second order in $J_\parallel$ they are given by [13] $g\mu_B H_{c1} = J_\perp - J_\parallel + J_\parallel^2/(2J_\perp)$ and $g\mu_B H_{c2} = J_\perp + 2J_\parallel$ with $g = 2.15$ for $H\|c^\star$ [14].
[13] M. Reigrotzki *et al.*, J. Phys. Condens. Matter **6**, 9235 (1994).
[14] B. R. Patyal *et al.*, Phys. Rev. B **41**, 1657 (1990).
[15] Ch. Rüegg, B. Thielemann, K. Krämer (unpublished).
[16] As the Schottky formula (2) is only valid up to first order in $J_\parallel$, we neglect here for consistency the second order in the $J_\parallel$ contribution in the formula for H_{c1} [12], yielding $J_\perp/k_B = 13.2$ K and $J_\parallel/k_B = 3.4$ K.
[17] G. Chaboussant *et al.*, Eur. Phys. J. B **6**, 167 (1998).
[18] F. Mila, Eur. Phys. J. B **6**, 201 (1998).
[19] K. Totsuka, Phys. Rev. B **57**, 3454 (1998).
[20] S. Sachdev *et al.*, Phys. Rev. B **50**, 258 (1994).
[21] A first-order transition is expected when the critical contribution to compressibility is comparable to the one from the lattice κ_L. An order of magnitude estimate shows that this occurs at a temperature $T_c \sim \frac{\gamma^4 V_D^2}{8\pi^2 k_B J_\parallel \kappa_L^2} \simeq 10^{-7}$ K, where we used $\kappa_L^{-1} \sim 10$ GPa. However, the first-order instability might be prevented by the onset of Néel order due to interladder coupling [15,22].
[22] T. Lorenz, F. Anfuso, M. Garst, A. Rosch (to be published).